Journal of New Technology and Materials
JNTM
Vol. 04, N°01 (2014)41-45

OEB Univ. Publish. Co.

The effect of bath temperature on the electrodeposition of zinc oxide nanostructures via nitrates solution

Loubna Mentar*, Hala Lahmar, Mohamed Redha Khelladi and Amor Azizi

Laboratoire de Chimie, Ingénirie Moléculaire et Nanostructures, Université Sétif-1, 19000, Algeria

Received: 30 April 2014, accepted 26 May 2014

Abstract

Zinc oxide (ZnO) nanostructures were electrodeposited onto ITO coated glass substrates from nitrate medium at different temperatures. The electrochemical deposition process was analyzed and the characteristics of the nanostructures were discussed. The electrochemical results showed that the deposition temperature had an important effect on the current density and the film morphology. From the Mott-Schottky measurements, the flat-band potential and the donor density for the ZnO
nanostructure are determined. The morphological, structural and optical properties were studied by scanning electron microscopy (SEM), x-ray diffraction techniques (XRD) and spectrophotometer in the ultraviolet UV–visible region. SEM images demonstrated that the morphology of ZnO nanostructures depend greatly on the bath temperature. The XRD patterns revealed the formation of phase-pure ZnO nanostructure with hexagonal wurtzite phase. The optical transmittance spectrum gave a high transmittance of 82 % at low temperatures, and the optical band-gap (E_g) of the ZnO nanostructures was between 3.25~3.49 eV.

Keywords: Electrodeposition, ZnO nanostructures, Mott-Schottky, morphology, structure.

1. Introduction

The synthesis of semiconductor crystals with well-defined shapes, sizes, and structures has attracted extraordinary interest in order to realize their unique properties that not only depend on their chemical composition, but also on their shape, structure, phase, size, and size distribution [1, 2]. Zinc oxide (ZnO) is one of the most promising materials for nanotechnology due to its range of potential applications such as sensors, photovoltaic cells, light-emitting diodes and nanogenerators. Among various synthesis methods, electrochemical deposition represents a simple and inexpensive solution based method for synthesis of semiconductor nanostructures. In effect, electrodeposition of ZnO is a versatile growth method and many various nanostructures with a range of morphologies can be easily designed by the technique [3]. Consequently, in recent years, there has been extensive interest in synthesizing various ZnO nanostructures, including nanowires, nanoribbons and nanotubes; the nanostructures growth was controlled by deposition parameters such as electrolyte bath composition, pH, deposition potential or deposition current density and bath temperature [4]. Consequently, in this paper, we report on the influence of deposition temperature on the properties of ZnO nanostructures.

2. Experimental Details

ZnO nanostructures were prepared by electrochemical deposition onto indium doped tin oxide (ITO) glass coated substrates with an exposed area of 1 x 2 cm^2 (10–20 Ω/cm^2 sheet resistance). All the depositions were made in a three-electrode electrochemical cell with the substrate as the working electrode (ITO), a Platinum wire as a counter electrode, saturated calomel electrode (SCE) as reference. The ITO substrate was first degreased in acetone and ethanol by ultrasonication for 15 min, and lastly well rinsed with distilled water. The electrodeposition of ZnO nanostructures and cyclic voltammetry (CV) measurements were carried out using, a computer controlled potentiostat/galvanostat (Voltalab 40) as a potential source. The electrolyte consisted of a solution contained 0.1 M zinc nitrate with 1 M KNO_3. The pH of solution is fixed at 6,5. Electrodeposition was performed at different temperatures ranging from 30 to 70 °C, without stirring. The ZnO nanostructure/electrolyte capacitance was measured at an AC frequency of 20

Hz using a Voltalab 40 Model PGZ301. Little frequency dispersion was observed for the measured capacitances in the frequency region 5–5000 Hz. The surface morphology and microstructure of the ZnO nanostructures were examined using Quanta 200 scanning electron microscope (SEM). Phases identification and crystallographic structure determination were carried out using XRD on a Philips X-pert pro diffractometer with $CuK\alpha_1$ radiation (λ = 1.5418 Å) in the θ- 2θ geometry. The optical transmittance spectra were obtained with a SHIMADZU 2401PC spectrophotometer in the ultraviolet UV–visible region. The spectra were corrected for glass substrates.

3. Results

3.1. *Electrochemical study*

In this work, the applied potential was fixed at -1.3 V vs. SCE, and [Zn^{2+}] at 0.1M and bath temperature were changed to systematically examine the electrochemical, morphological and structural properties of electrodeposited ZnO. In order to verify the influence of temperature on the electrochemical behavior of the electrodes in the electrodeposition bath, the cyclic voltammetry was performed. Fig. 1 shows the voltammograms obtained from 0.1 M zinc nitrate aqueous solution at different temperatures. It is clear that the intensity of the cathode current increases with the temperature of the electrolytic bath. Indeed, in the range from 30 and 70 °C, the intensity varies from -1.21 to -3.38 mA/cm^2, respectively. A change in the kinetics at the electrode can be mentioned as consequence of the shift of the peaks of Zn reduction to more negative values of the potential [5]. The crystallization accompanied by dehydration may depend on the deposition temperature [6].

It's well established that the electrodeposition of ZnO is a three-stage process [7]. At the first stage, hydroxide ions are contributed from both $Zn(NO_3)_2$ and KNO_3. Chemical reactions taking place at the working electrode during the electrochemical deposition reaction of ZnO nanostructures are the following [8]:

$$NO_3^- + H_2O + 2e^- \rightarrow NO_2^- + 2OH^- \quad (1)$$

$$Zn^{2+} + 2OH^- \rightarrow Zn(OH)_2 \quad (2)$$

$$Zn(OH)_2 \rightarrow ZnO\downarrow + H_2O \quad (3)$$

This result in the following total reaction:

$$Zn^{2+} + NO_3^- + 2e^- \rightarrow ZnO + NO_2^- \quad (4)$$

Referring to Fig. 1, two reduction picks in the potential range of 0 and −1.4 V vs. SCE are observed. One corresponds to reduce of nitrate ions (NO_3^-) to hydroxyl ions (OH^-) (eq. 1) which occurs around −0.65 V vs. SCE. The other reaction reduces Zn^{2+} ions to metallic Zn (eq. 2) which occurs below around −1.0 V. When the applied potential is around −0.7 V, OH^- ions are produced in the deposition solution, which in turn react with Zn^{2+} ions in the solution to form ZnO (eq.3)

The conduction type, the flat band (E_{fb}), and the estimated donor densities of ZnO were determined using Mott–Schottky (M-S) measurements with $1/C^2$ vs. E at a fixed frequency of 20 k Hz. The capacitance-potential measurements are presented as an M-S plot following the equation below [9]:

$$\frac{1}{C^2} = \frac{2}{N_D e \varepsilon_0 \varepsilon}\left[(E - E_{fb}) - \frac{kT}{e}\right] \quad (5)$$

where C is the space charge capacitance in the semiconductor; N_d is the hole carrier density; e is the elemental charge value; ε_0 is the permittivity of the vacuum; of free space; (8.85 9 10^{-14} F cm^{-1}); ε is the relative permittivity of the semiconductor (ε of ZnO is 8.5); E is the applied potential, E_{fb} is the flat band potential, T is the temperature, and k is the Boltzmann constant.

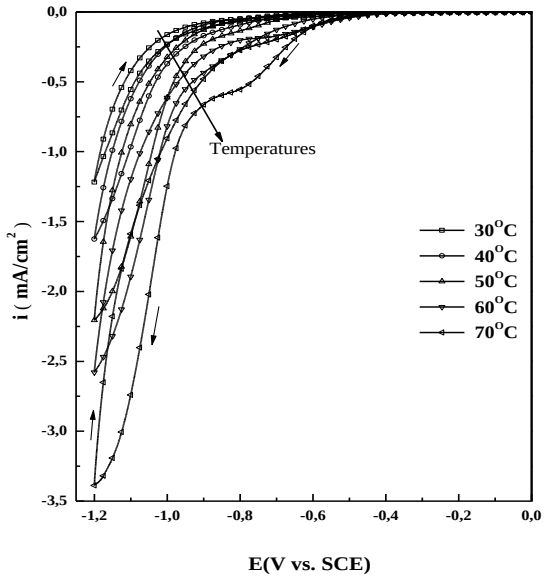

Fig. 1 Cathodic scan of 0.1 M $Zn(NO_3)_2$ with 1 M KNO_3 aqueous solution on a ITO electrode at pH 6.5 at different bath temperatures from 30 to 70 °C.

By plotting the $\frac{1}{C^2}$ versus E, the donor density and the flat-band potential of an n-type semiconductor can be obtained from the slope ($=\frac{2}{\varepsilon\varepsilon_0 e N_D}$) and intercept at $C = 0$. Thus from Fig. 2, the flat-band potential and the donor density of an n-type semiconductor of ZnO deposited at different temperatures are summarized in Table 1. As indicated, the estimated donor densities are found to decrease with increasing deposition temperature.

Table 1: Donor density and flat band potential (E_{fb}) calculated from Mott-Schottky equation.

T (°C)	E_{fb} (V)	N_D ($\times 10^{20}$ cm^{-3})
30	-0.870	4.96
40	-1.029	4.76
50	-0.800	2.58
60	-1.148	2.15
70	-1.026	4.31

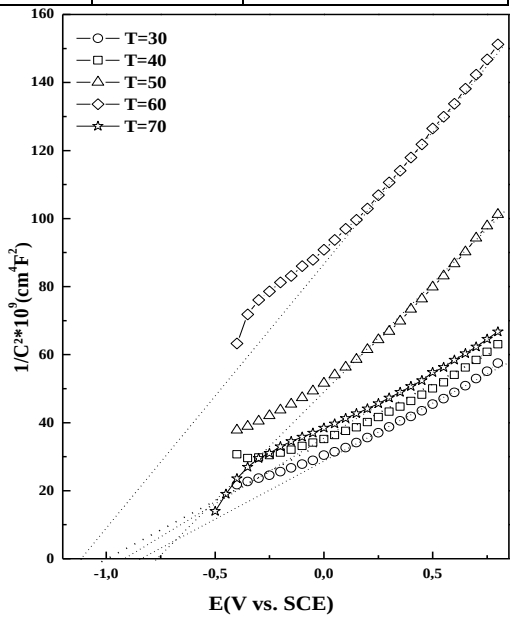

Fig. 2 Mott-Schottky plot for electrodeposited ZnO nanostructures of 0.1 M $Zn(NO_3)_2$ + 1M KNO_3 solution obtained at 20 Hz at different bath temperatures (30 → 70 °C). The corresponding flat band potential values are indicated. The lines were simply drawn through the data points.

3.2. Morphology

The morphology of deposited ZnO nanostructures was observed by SEM (Fig. 3), which exhibited different morphologies. The surface morphologies are found to change considerably as the deposition temperature is increased. For the growth at 30 °C, very thin nanosheet structures grown on the substrate are obtained as illustrated in Fig. 3a. When the deposition temperature is increased from 40 to 70 °C, some sheet structures become quite bigger as shown in Fig. 1b, d and e. In particular, for the deposition temperature around 50 °C, the surface morphology of deposit exhibited entangled nanostructures (Fig. 3c); these morphology is observed in the literature [10, 11].

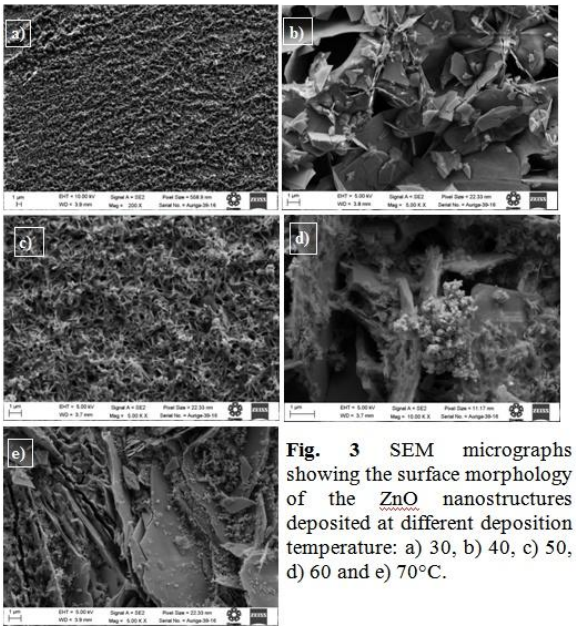

Fig. 3 SEM micrographs showing the surface morphology of the ZnO nanostructures deposited at different deposition temperature: a) 30, b) 40, c) 50, d) 60 and e) 70°C.

3.3. Structural analysis

Fig. 4 shows the XRD patterns in the 2θ range of 25 to 75 of the ZnO nanostructures prepared at different temperatures. All samples are polycrystalline with hexagonal wurtzite structure (JCPDS 01-076-0704). Also, these patterns showed that the structure of the deposits was sensitive to the bath temperature used for the deposition of ZnO nanostructures. From the XRD patterns the crystallinity of ZnO was improved by increasing deposition temperature and as consequence intensities of other peaks also increase. In particular, the nanostructure deposited at 70 °C has a strong (101), (100) and (002) orientations; signed for height crystallinity. The average crystallite size was estimated from the full width at half- maximum

(FWHM) values of diffraction peaks using the Scherrer formula [12]:

$$D = \frac{0.9\lambda}{\beta cos\theta} \quad (6)$$

where D is the crystallite size, β is the broadening of the diffraction line measured at FWHM, λ is the x-ray wavelength (1.5406 Å) used and θ is the diffraction angle.

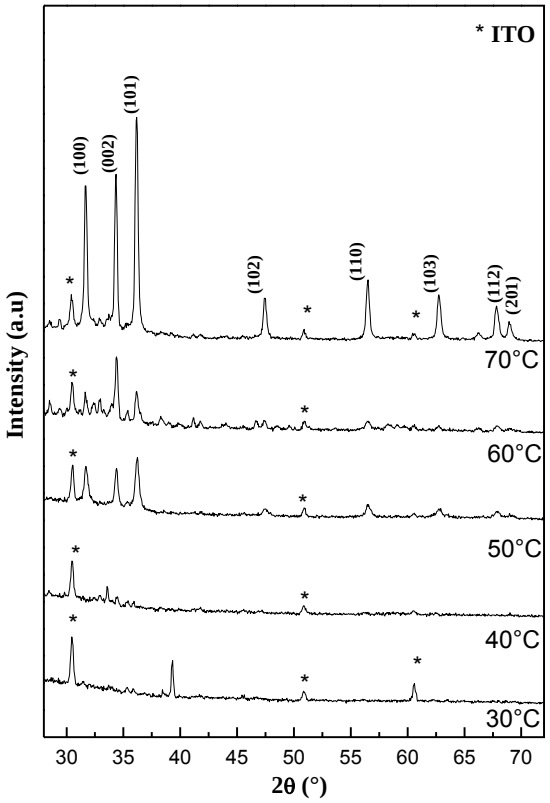

Fig.4 XRD patterns of ZnO nanostructures deposited at various temperature from 30 to 70°C. XRD peaks of ITO substrate are marked by *.

The crystallite size, calculated after correcting for instrumental broadening, along the (002) peak ranges from 55 to 64 nm. From these values, it is observed that the average crystallite size increases with the bath temperature.

3.4. *Optical properties*

The optical transmission spectra recorded in the range of 200 to 800 nm of the ZnO nanostructures deposited at different temperature are shown in Fig. 5.

The values of the transmission obtained vary from 82 to 74 % with increasing deposition temperature. It may be seen from this entire figure that all the prepared ZnO nanostructures films exhibited high optical transmittance (> 70 %) in the visible region. The decrease of the film transparency with the increase of temperature can be explained by the increasing of the thickness of nanostructures at high temperature [13].

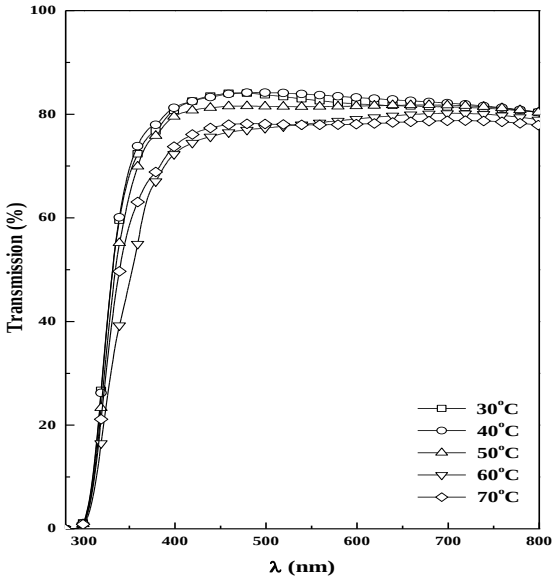

Fig. 5 Transmission spectra of the ZnO nanostructers deposited at different temperature.

The Tauc's plot were drawn to determine the energy band gap values of the deposited films, the nature of transition is determined using the following equation [14],

$$\alpha h\upsilon = A(h\upsilon - E_g)^n \quad (7)$$

where α is absorption coefficient in cm^{-1}, hν is photon energy, E_g is an energy gap, A is energy dependent constant and n is an integer depending on the nature of electronic transitions. For the direct allowed transitions, n has a value of 1/2 while for the indirect allowed transitions, n = 2. The value of band gap at different deposition temperature was found to be in the range of 3.25-3.49 eV. These values decrease with increasing the temperature deposition.
It can be attributed to improvement in the crystallinity with temperature as supported by XRD studies.

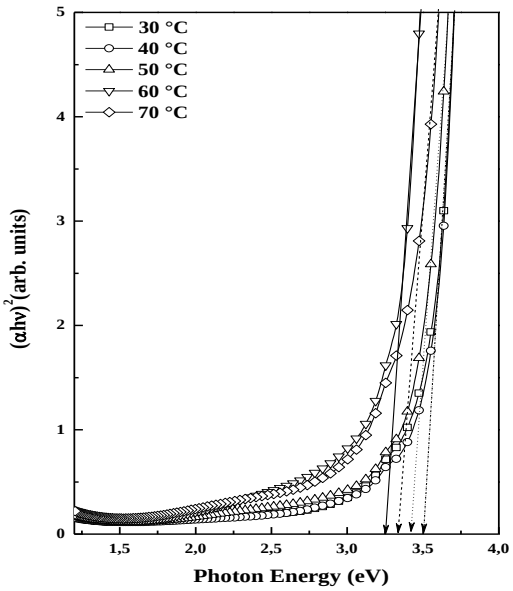

Fig. 6 Plot $(\alpha h\upsilon)^2$ versus $h\upsilon$ for ZnO nanostructures films deposited at different temperature. The band gap values obtained by extrapolating the linear part of the curves are also shown.

These results clearly show that the morphology and crystallite size of the ZnO deposits plays a very important role in the control of the light scattering. Indeed, nanostructures deposited at high temperatures, relatively large size (> 60 nm) are very interesting for inducing an effective dissemination throughout the wavelength range of visible light. This can be very important for their application in nanostructured solar cells.

4. Conclusion

We have studied the effects of bath temperature on the electrodeposition of nanostructures from nitrate medium. The carrier density of ZnO nanostructures decreased from 4.96×10^{20} to 2.15×10^{20} cm^{-3} with increasing deposition temperature. The nanostructures with different morphology and high crystanillity could be obtained by increasing the temperature. The optical transmittance spectrum gave a relatively high transmittance (≈ 80 %) and the optical band-gap of the ZnO nanostructures was found to increase with temperature and to be in the range of 3.25-3.49 eV.

References

[1] X. Lan, J. Y. Zhang, H. Gao, T. M. Wang. CrystEngComm 13 (2011) 636.
[2] S. Chatterjee, S. Gohil, B. Chalke, P. Ayyub, 9 (2009) 4792.
[3] M.R. Khelladi, L. Mentar, M. Boubatra, A. Azizi, Mater. Lett. 67 (2012) 331.
[4] M. R. Khelladi, L. Mentar, A. Beniaiche, L. Makhloufi, A.Azizi.,J Mater Sci: Mater Electron, 24 (2013) 153.
[5] S. Otani, J. Katayama, H. Umemoto, M. Matsuoka, J. Electrochem. Soc. 153 (2006) C551.
[6] Belavalli E. Prasad, P. Vishnu Kamath, S. Ranganath, J Solid State Electrochem 16 (2012) 3715.
[7] T. Yoshida, D. Komatsu, N. Shimokawa, H. Minoura, Thin Solid Films, 451 (2004) 166.
[8] S.J. Limmer, E.A. Kulp, J. A. Switzer, Langmuir, 22 (2006) 10535.
[9] S.R. Morrison, Electrochemistry at semiconductor and oxidized metal electrodes (Plenum Press, New York, 1980).
[10] K. Wuaz, J. biao Cuib, ECS Solid State Letters, 2 (2013) 8742.
[11] T. Singh, D. K. Pandya, R. Singh, International Conference on Physics of Emerging Functional Materials (PEFM-2010).
[12] A.D. Krawitz, Introduction to Diffraction in Materials Science and Engineering, Wiley-VCH, April 2001.
[13] R. Mariappan, V. Ponnuswamy, P. Suresh, Superlattice Microst 52 (2012) 500.
[14] J. Tauc. Optical Properties of Solids 22, F. Abeles, Ed., North Holland Pub, Amsterdam, (1970).